



Introduction of organic/inorganic Fe₃O₄@MCM-41@Zr-piperazine magnetite nanocatalyst for the promotion of the synthesis of tetrahydro-4*H*-chromene and pyrano[2,3-*d*]pyrimidinone derivatives

Reyhaneh Pourhasan-Kisomi¹ | Farhad Shirini¹ | Mostafa Golshekan²

¹Department of Chemistry, College of Sciences, University of Guilan, Rasht 41335-19141, Iran

²Neuroscience Research Center, Department of Pharmacology, Guilan University of Medical Science, Rasht, Iran

Correspondence

Farhad Shirini, Department of Chemistry, College of Sciences, University of Guilan, Rasht, 41335-19141, Iran.

Email: shirini@guilan.ac.ir

Fe₃O₄@MCM-41@Zr-MNPs modified with piperazine is easily prepared and characterized using Fourier transform infrared spectroscopy (FT-IR), X-ray powder diffraction (XRD), N₂ adsorption-desorption, Transmission electron microscopy (TEM), Energy-dispersive X-ray (EDX), Vibrating sample magnetometry (VSM) and Thermogravimetric analysis (TGA) techniques. The characterization results showed that Zr highly dispersed in the tetrahedral environment of silica framework and piperazine is successfully attached to the surface of the nanocatalyst in connection with zirconium. The prepared nanosized reagent (10–30 nm), shows excellent catalytic activity in the synthesis of tetrahydro-4*H*-chromene and pyrano[2,3-*d*]pyrimidinone derivatives. All reactions are performed under mild and completely heterogeneous reactions conditions in high yields during short reaction times. On the other hand and due to its superparamagnetic nature the catalyst can be easily separated by the application of an external magnetic field and reused for several times.

KEYWORDS

Fe₃O₄@MCM-41@Zr-MNPs, piperazine, pyrano[2,3-*d*]pyrimidinone, superparamagnetic, tetrahydro-4*H*-chromene

1 | INTRODUCTION

Silica mesoporous compounds are defined as natural and synthetic compounds with a pore size of 2–50 nm, which are classified between the two micro and macroporous categories. The unique properties of silica mesoporous materials like MCM-41 such as high surface area (~1000 m².g⁻¹), large pore size (2–50 nm), narrow pore size distribution, high thermal stability and the possibility of using them in a wide range of applications such as catalization, isolation, photocatalysis, sensors, absorption, etc. has focused many researchers and scientists studies on this category of nanoporous materials.^[1–7]

Tetrahydro-4*H*-chromenes and their derivatives are of remarkable interest because of their wide range of biological properties, such as spasmolytic, diuretic, anti-coagulant, anti-cancer and anti-anaphylactic activities.^[8,9] In addition, they can be used as cognitive enhancers, for the treatment of neurodegenerative disease, including Alzheimer's disease, amyotrophic lateral sclerosis, Huntington's disease, Parkinson's disease, AIDS associated dementia and Down's syndrome as well as for the treatment of schizophrenia and myoclonus.^[10,11] 4*H*-Pyrans also constitute the structural unit of a series of natural products. Finally, a number of 2-amino-4*H*-pyrans are useful as photoactive materials.^[12] They are

often used in cosmetics, pigments and utilized as potential agrochemicals.^[13]

Pyrano[2,3-*d*]pyrimidinones are regular structural subunits in a variety of important natural products, including carbohydrates, alkaloids, polyether antibiotics, pheromones, and iridoids. These compounds have received considerable attention over the past years due to their wide range of biological activities such as anti-tumor, anti-bacterial, anti-hypertensive, hepatoprotective, cardioprotective, vasodilator, bronchodilators and anti-allergic activities.^[14] Some of them exhibit anti-malarial, anti-fungal, analgesics and herbicidal properties.^[15]

Because of the aboved mentioned very important characteristics, various synthetic procedures have been reported for the synthesis of tetrahydro-4*H*-chromenes and pyrano[2,3-*d*]pyrimidinones using acidic and basic catalysts such as metformin-modified silica-coated magnetic nanoparticles (MNPs) (Fe₃O₄/SiO₂-Met),^[16] Fe₃O₄@SiO₂/DABCO,^[8] γ-Fe₂O₃@HAp Si(CH₃)₃AMP,^[10] high surface area MgO,^[17] *N*-methylimidazole,^[9] tetrabutylammonium bromide,^[18] trisodium citrate,^[19] *p*-dodecylbenzenesulfonic acid,^[11] poly (4- vinylpyridine),^[20] potassium phthalimide-*N*-oxyl,^[21] [cmmim]Br and [cmmim][BF₄],^[22] choline chloride (ChCl),^[23] starch solution,^[24] (diacetoxyiodo)benzene (DIB)^[25] (for the synthesis of tetrahydro-4*H*-chromenes), diammonium hydrogen phosphate (DAHP),^[26] *L*-proline,^[27] KAl(SO₄)₂·12H₂O (alum),^[28] tetrabutylammonium bromide (TBAB),^[29] DABCO,^[30] sulfonic acid nanoporous silica (SBA-Pr-SO₃H),^[31] Al-HMS-20,^[32] Nano- sawdust- OSO₃H,^[33] ZnO-supported copper oxide,^[14] succinimidinium hydrogensulfate ([H-Suc] HSO₄)^[34] and [H₂-DABCO] [H₂PO₄]₂^[35] (for the synthesis of pyrano[2,3-*d*]pyrimidinones). However, aforementioned methods suffer from some drawbacks such as low yields, extended reaction times, harsh reaction conditions, tedious work-up procedures, toxic solvents and application of the expensive or unavailable catalyst. Moreover, the main disadvantages of most of the existing methods are that the catalysts are decomposed under aqueous work-up conditions and their recoveries are often impossible. Therefore, the introduction of new catalytic systems which in them the above mentioned difficulties be excluded is still in demand.

The susceptibility of transition elements to mediate organic synthesis constitutes one of the most efficient strategies to attain both selectivity and efficiency in synthetic chemistry.^[36] Zirconium pertains to group IV transition elements that can be considered as efficient catalysts due to easy availability, low cost and low toxicity. Zirconium (IV) compounds possess a high coordinating ability due to the higher charge-to-size value of Zr⁴⁺ compared to most of the metal ions that allows displaying a good *Lewis* acid behavior and high catalytic activity.

Moreover, many zirconium salts are now commercially available or described in the literature.^[37,38] Despite its advantages, the utility of zirconium (IV) compounds as *Lewis* acids for organic reactions has not been exploited to a greater extent largely compared to other transition metals.^[39–41] With increasing environmental concerns and the need for efficient and green *Lewis* acid catalysts for various useful organic transformations, the interest in zirconium and its compounds has increased in last decade.^[42]

In order to increase the availability of active sites of zirconium to compensate its low surface area, it can be proposed to introduce zirconium into the framework of molecular sieves pending their synthesis as co-condensation or direct ones, by analogy with what had been made with many other elements. In this type of mesoporous mixed metal materials, metals are highly dispersed and more active sites can be available.^[43,44] Moreover, the thermal and hydrothermal stability can be increased.^[45] In addition, to improve zirconium catalytic activity in organic reactions, functionalization by organic amine groups like piperazine as a basic functional group seems to be a good idea.

In the other hand, to protect the environment and in order to avoid manual attempts to filtrate and purify catalysts, it is urgently needed to improve the methods that can lead to the recovery and reuse of these nanocomposites at low concentrations in complex matrices. To do this, heterogenization of the catalyst in the form of magnetic nanoparticles leads to catalyst recovery using an external magnetic field and increasing the efficiency of nanocatalysis in the next reuses.

On the basis of the previously mentioned drawbacks on the synthesis of tetrahydro-4*H*-chromenes and pyrano[2,3-*d*]pyrimidinones, in order to introduce more effective, useful and environmentally benign method for the synthesis of these compounds and in continuation of our previous reports on the application of different acidic and basic catalysts, particularly zirconium based and supported reagents in organic transformations,^[46–49] we were interested to prepare Fe₃O₄@MCM-41@Zr-piperazine-MNPs (Figure 1) and investigate its applicability in the promotion of the synthesis of the above mentioned target molecules.

2 | EXPERIMENTAL

2.1 | Materials

All chemicals including FeCl₃·6H₂O, FeCl₂·4H₂O, tetraethylorthosilicate (TEOS), cetyl trimethylammonium bromide (CTAB), NaOH, NaF, ZrOCl₂·8H₂O, piperazine, benzaldehyde derivatives, dimedone, malononitrile, and

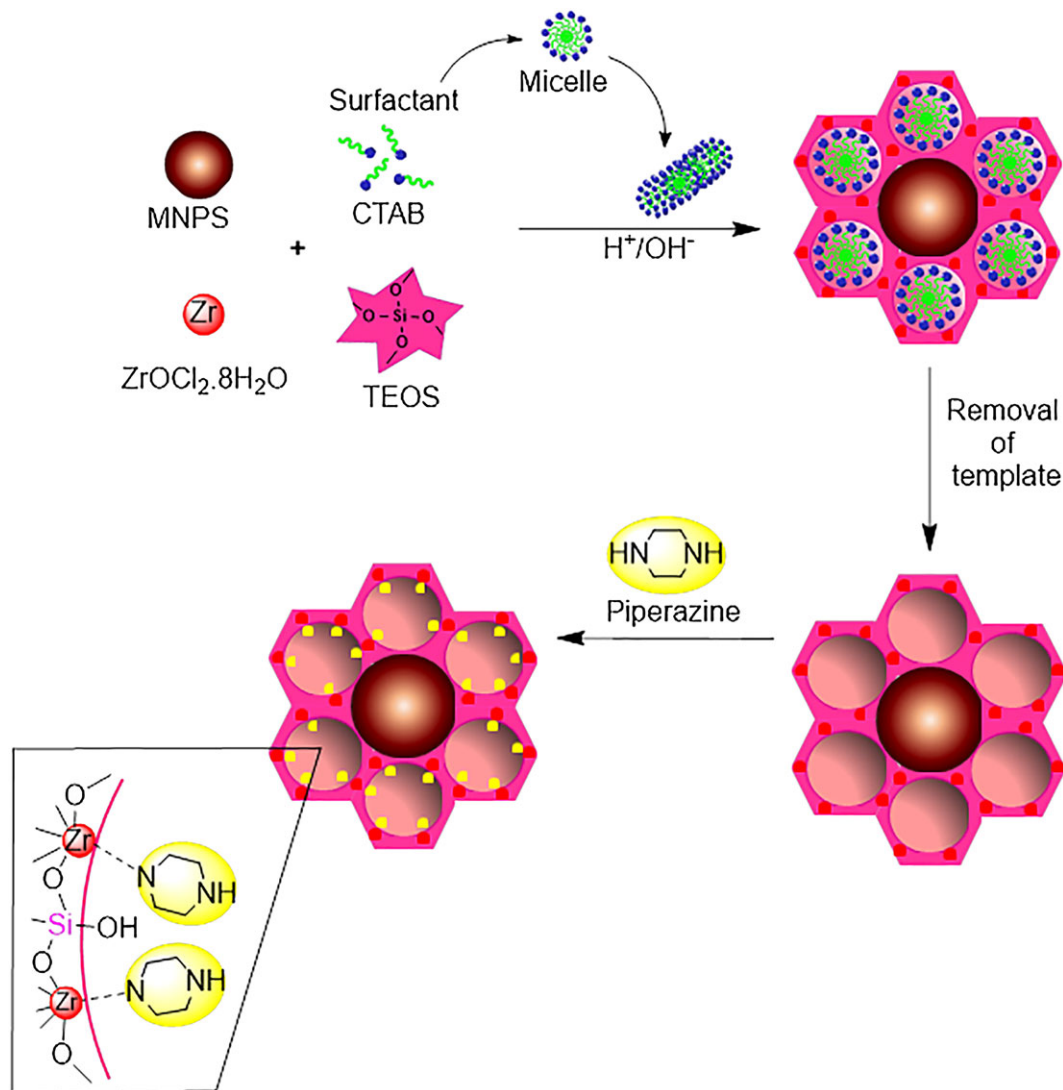


FIGURE 1 Preparation of Fe₃O₄@MCM-41@Zr-piperazine-MNPs

barbituric acid were purchased with high purity from Merck chemical company (Munich, Germany). All solvents were prepared from Merck (Munich, Germany) and in order to minimize the absorption of atmosphere moisturize, in addition to getting distilled before being used, they were kept sealed in airtight bottles as well.

2.2 | Characterization techniques

All products were characterized by comparing their physical constants, and IR and NMR spectroscopy with authentic samples and those reported in the literature. The purity determination of the substrate and reaction monitoring was accompanied by thin-layer chromatography (TLC) on a silica gel Polygram SILG/UV 254 plate. Measuring Melting points were accomplished using electrothermal IA9100 melting point apparatus in capillary tubes. The quality and composition of pelletized samples of synthesized nanoparticles were characterized

via Fourier transform infrared spectroscopy (FT-IR) measurements by Perkin-Elmer Spectrum BX series in the range of 400–4000 cm⁻¹. Analyzing the crystal phases and crystallinity of synthesized MNPs were accomplished by Philips PW1730 (Netherlands) instrument in the range of 0.7°–80° (2 θ). Iron Scanning electron microphotographs (FESEM) and Energy Dispersive Spectrometer (EDS) was performed on a TESCAN MIRA II (Czech Republic) device to study the size and morphology of particles. The pore volume, the BET surface area, and the average pore size obtained before and after the modification was characterized by N₂ adsorption/desorption which was carried out at 77° K on a BELSORP-mini II apparatus using nitrogen. The samples were outgassed at 393° K and 1 mPa for 12 h before adsorption measurements. Thermogravimetric analysis (TGA) and differential thermal analysis (DTA) was carried out with a Q600 TGA analyzer under Argon atmosphere from 25 to 1200 °C with a heating rate of 20 °C min⁻¹ over. The

magnetic properties were determined using vibrating sample magnetometry (VSM; Lake Shore 7200 at 300 kVsm). ^1H NMR and ^{13}C NMR spectra were determined on Bruker AV-400 using TMS (0.00 ppm) as internal standard and DMSO- d_6 as solvent.

2.3 | Preparation of the catalyst

2.3.1 | Preparation of Fe_3O_4 -MNPs

The synthesis of Fe_3O_4 -MNPs was accomplished according to our previous method with minor modification.^[50] In this way, 6.3 g $\text{FeCl}_3 \cdot 6\text{H}_2\text{O}$, 4.0 g $\text{FeCl}_2 \cdot 4\text{H}_2\text{O}$ and 1.7 ml HCl (12 mol l^{-1}) were dissolved in 50 ml of deionized water in a beaker. Then, the solution was degassed with argon gas and heated to 80 °C in a reactor. Concomitantly, 250 ml of a 1.5 mol l^{-1} ammonia solution was slowly added to the solution under argon gas protection and vigorous stirring (1000 rpm). After completion of the reaction, the resultant black solid of Fe_3O_4 -MNPs was separated from the reaction medium using an external magnet, and after that was washed four times with 500 ml double distilled water. Finally, the obtained Fe_3O_4 -MNPs were resuspended in 500 ml of degassed deionized water. The concentration of the obtained product of Fe_3O_4 -MNPs was determined as 6.2 mg ml^{-1} .

2.3.2 | Preparation of Fe_3O_4 @MCM-41@Zr-MNPs

To synthesize Fe_3O_4 @MCM-41, we followed the method described by Golshekan *et al.*^[50] As for the introducing of Zr in the MCM-41 framework, we followed the method reported by Chien *et al.*^[51] and Yang *et al.*^[44,52] with a little modification. Typically, 2.186 g of cetyltrimethylammonium bromide (CTAB), 1.461 g of NaCl and 1.5 g of the synthesized MNPs were mixed in 130 g of H_2O at room temperature, and 0.6404 g of $\text{ZrOCl}_2 \cdot 8\text{H}_2\text{O}$ was then added to the above solution. The resulting solution was stirred vigorously for 1 h, followed by the addition of 5.2 g of tetraethyl orthosilicate (TEOS). After being stirred for 1 day, the mixture was transferred to an autoclave and hydrothermally treated in an oven at 100 °C for 24 h under static conditions. The solid product was separated using an external magnetic field, washed thoroughly with distilled water, and dried at 120 °C for 5 h. Finally, the template was removed from the as-synthesized Fe_3O_4 @MCM-41@Zr-MNPs by calcination of the synthesized particles at 550 °C for 6 h. It's notable that based on Yang and his coworker's researches,^[52] at a Zr/Si ratio of 3/40, Zr-MCM-41 functionalized by the amine group exhibits the best efficiency.

2.3.3 | Preparation of piperazine -functionalized Fe_3O_4 @MCM-41@Zr-MNPs

For the synthesis of the functionalized Fe_3O_4 @MCM-41@Zr-MNPs with amine groups, we followed the procedure reported by Yue *et al.*^[53] and Yang *et al.*^[52] with minor modification. Typically, 2.186 g of piperazine was dissolved in 10 g of methanol, and then 0.3 g of calcined Fe_3O_4 @MCM-41@Zr-MNPs was added to the solution. The resulting slurry was continuously stirred at room temperature for 5 h and then dried at 70 °C for the removal of solvent, followed by further drying at 100 °C for 1 h.

2.4 | General procedure for the synthesis of tetrahydro-4H-chromene derivatives

To prepare tetrahydro-4H-chromene derivatives, an equimolar mixture of an aromatic aldehyde (1 mmol), malononitrile (1.2 mmol), and dimedone (5,5-dimethyl-1,3-cyclohexanedione) (1 mmol), and Fe_3O_4 @MCM-41@Zr-piperazine nanocatalyst (0.03 g) was dissolved in 3 ml aqueous ethanol (7:3) and stirred at 75 °C for appropriate time. When the reaction was completed as indicated by TLC (*n*-hexane: ethyl acetate; 6:4), the mixture was purified with ethanol. Afterward, in the presence of a magnetic stirrer bar, Fe_3O_4 @MCM-41@Zr-piperazine nanocatalyst was separated and the reaction mixture turned clear. Finally, the crude product was recrystallized from EtOH to give a pure product.

2.5 | General procedure for the synthesis of pyrano[2,3-d]pyrimidinone derivatives

Fe_3O_4 @MCM-41@Zr-piperazine nanocatalyst (0.03 g) was added to a mixture of the aromatic aldehyde (1 mmol), malononitrile (1.2 mmol) and barbituric acid (1 mmol) in 3 ml aqueous ethanol (1.5:1.5). Then the mixture was heated at 80 °C while was monitored by TLC (*n*-hexane: ethyl acetate; 7:3). After completion of the reaction, the mixture was recrystallized with ethanol. The magnetic nanocomposites were then separated in the presence of a magnetic stirring bar; the reaction mixture became clear. The crude product was recrystallized from ethanol to give a pure product.

Spectral (^1H and ^{13}C NMR) data of the compounds 4o and 4p from Table 4 are presented below:

4,4'-(1,4-Phenylene)bis(2-amino-7,7-dimethyl-5-oxo-5,6,7,8-tetrahydro-4H-chromene-3-carbonitrile) (4o): m.p. 266–268 °C; IR (neat) ν = 3450, 3332, 3185, 2958, 2933, 2229, 1661, 1584 cm^{-1} ; ^1H NMR (DMSO- d_6 , 400 MHz): δ = 0.985 (s, 6H, 2CH₃), 1.035 (s, 6H, 2CH₃), 2.14–2.38 (m, 4H), 2.45–2.56 (m, 4H), 4.14 (s, 2H), 6.98 (s, 4H),

2NH₂), 7.04 (s, 4H, Ar-H); ¹³C NMR (DMSO-d₆, 100 MHz): δ = 27.4, 27.6, 28.6, 32.3, 35.4, 50.4, 58.8, 113.1, 120.2, 127.4, 143.3, 159.0, 163.1, 196.1 ppm.

4,4'-(1,3-Phenylene)bis(2-amino-7,7-dimethyl-5-oxo-5,6,7,8-tetrahydro-4H-chromene-3-carbonitrile) (4p): m.p. 240–242 °C; IR (neat) ν = 3450, 3384, 3327, 3213, 2961, 2197, 1664, 1601, 1367 cm⁻¹; ¹H NMR (DMSO-d₆, 400 MHz): δ = 0.955 (s, 6H, 2CH₃), 1.057 (s, 6H, 2CH₃), 2.045 (d, J_{AB} = 17.4 Hz, 2H), 2.28 (d, J_{AB} = 17.4 Hz, 2H), 2.38 (d, J_{AB} = 17.4 Hz, 2H), 2.59 (d, J_{AB} = 17.4 Hz, 2H), 4.113 (s, 2H), 6.80 (s, 1H, Ar), 6.92 (s, 4H, NH), 7.01 (dd, 2H, J_1 = 7.6 Hz, J_2 = 1.6 Hz), 7.192 (t, 1H, J = 7.6, Ar) ppm; ¹³C NMR (DMSO-d₆, 100 MHz): δ = 19, 26.9, 29.3, 32.1, 35.7, 50.3, 56.5, 58.6, 113.2, 120.1, 125.1, 126.2, 128.3, 145.5, 159, 162.9, 195.9.

3 | RESULT AND DISCUSSION

3.1 | Characterization of the catalyst

3.1.1 | FT-IR analysis

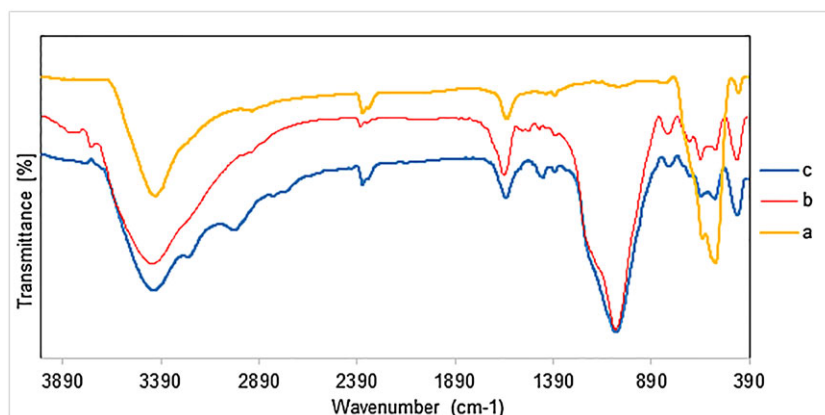
Comparison of the FT-IR spectra of the Fe₃O₄-MNPs, Fe₃O₄@MCM-41@Zr-MNPs and Fe₃O₄@MCM-41@Zr-piperazine-MNPs confirm the structure of the synthesized nanoparticles (Figure 2). For the bare MNPs, Fe₃O₄ usually shows bands at ~560 and 450 cm⁻¹, from Fe–O vibrations at tetrahedral and octahedral sites, respectively.^[54] In the FT-IR spectra of the finally prepared reagent, there are stretching vibrations of O–H bonds at ~3435 cm⁻¹ and bending vibrations of these bonds at 1635 cm⁻¹.^[55] An intense peak at 1000–1250 cm⁻¹ corresponded to the Si–O stretching vibrations in the amorphous silica shell.^[50] Also, the external vibrations of SiO₄ chains can be observed at ~1200 and 800 cm⁻¹.^[55] In this spectra, the angular bending of Si–O units (450 cm⁻¹) is overlapped with the Fe–O vibrations.^[56,57] The band at 980 cm⁻¹ shows the fundamental vibrations of Zr–O–Si which overlaps with the Si–OH vibrations of

Fe₃O₄@MCM-41 nanoparticles.^[58] The broad strong bond which appears at 3230 cm⁻¹ is related to the N–H bond of piperazine and the bands at 2810 cm⁻¹ and 2950 cm⁻¹ are due to CH₂ stretching vibrations.^[59]

3.1.2 | Powder X-ray diffraction (XRD) analysis

X-ray diffraction (XRD) patterns of the mesoporous Fe₃O₄-MNPs showed peaks that could be indexed both mesoporous structure and MNPs (Figure 3). The Fe₃O₄-MNPs indicated peaks with 2 θ at 29.72°, 35.57°, 43.17°, 57.15° and 62.77° which are characteristic peaks of Fe₃O₄ and matched well with the XRD pattern of the standard Fe₃O₄ from Joint Committee on Powder Diffraction Standards (JCPDS No. 19–692).^[60] The three peaks with 2 θ at 1.5°–10° are characteristic peaks of MCM-41.^[50] The peaks resemble those of magnetite, indicates the presence of magnetite in the caves of the synthesized nanocomposites. In low angle region, Fe₃O₄@MCM-41@Zr-MNPs displayed an obvious diffraction peak around 0.8°–1°, characteristic of the Bragg plane reflection (100), and one poorly resolved diffraction peak around 2°–4°, indexed as (110) reflection, which indicates the presence of ordered mesostructure and the incorporation of Zr⁴⁺ in the framework of MCM-41 as a sufficient evidence.^[60] As a more precisely description, consistent with Yang *et al.* findings,^[44] after incorporation of ZrOCl₂ into the gels, ordered Zr-MCM-41 was obtained, with the explanation that the peak intensity of (100) plane gradually decreased and the diffraction peaks of (110) and (200) planes gradually disappeared with introducing of Zr, which meant that the ordering of Zr-MCM-41 samples decreased when Zr was introduced into the framework of Fe₃O₄@MCM-41-MNPs. With loading of piperazine, there is decrease of peak intensity as well as a shift of the (100) peak for Fe₃O₄@MCM-41@Zr-MNPs to the low angle degree for Fe₃O₄@MCM-41@Zr-piperazine-MNPs. The results are similar to that observed by Xu *et al.*^[61] upon

FIGURE 2 The FT-IR spectra of a) Fe₃O₄-MNPs b) Fe₃O₄@MCM-41@Zr-MNPs and c) Fe₃O₄@MCM-41@Zr-piperazine-MNPs



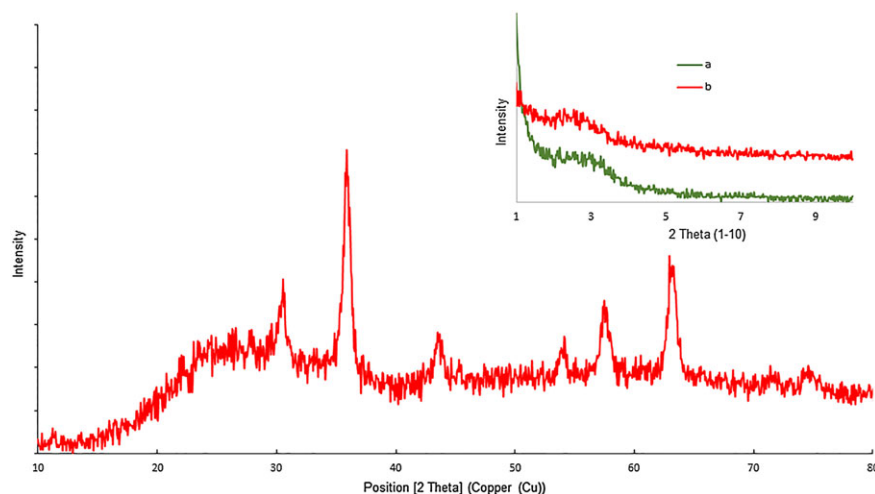


FIGURE 3 The XRD patterns of a) $\text{Fe}_3\text{O}_4@\text{MCM-41}@\text{Zr-MNPs}$ and b) $\text{Fe}_3\text{O}_4@\text{MCM-41}@\text{Zr-piperazine-MNPs}$

the loading of polyethyleneimine (PEI) onto MCM-41. Accordingly, The diffraction patterns of MCM-41 did not change after the piperazine was loaded, which indicated that the structure of MCM-41 was preserved. However, the intensity of the diffraction peaks of MCM-41 did change. After loading of piperazine, the intensity of the diffraction peaks of $\text{Fe}_3\text{O}_4@\text{MCM-41}@\text{Zr-MNPs}$ decreased, which was possibly caused by the pore filling by piperazine.

3.1.3 | BET analysis

The nitrogen adsorption/desorption isotherms of $\text{Fe}_3\text{O}_4@\text{MCM-41}@\text{Zr-MNPs}$ before and after modification with piperazine are shown in Figure 4. The isotherms correspond to type IV (in the IUPAC classification), which is typical of mesoporous materials,^[62] and further confirm that the piperazine was loaded into the pore channels of the MCM-41 support. The Brunauer-Emmet-Teller (BET) surface areas, total pore volume and Barret-Joyne-Halendu (BJH) pore diameter were $597.42 \text{ m}^2.\text{g}^{-1}$, $0.3912 \text{ cm}^3.\text{g}^{-1}$, and 2.6196 nm , respectively. After loading of piperazine, the mesoporous

pores were filled with piperazine, restricting the access of nitrogen into the pores at the liquid nitrogen temperature.^[61] The surface area was estimated to be $219.57 \text{ m}^2.\text{g}^{-1}$ and the residual pore volume of the $\text{Fe}_3\text{O}_4@\text{MCM-41}@\text{Zr-piperazine-MNPs}$ is only $0.3072 \text{ cm}^3.\text{g}^{-1}$. These results correlate with the pore filling effect of the piperazine which was also reflected by the XRD characterization. As we can see, the adsorption curve is identical to the desorption curve, which indicates that materials possess broad mesoporous structure.^[63] Although after piperazine impregnation, the BET surface and total pore volume area were reduced, high surface areas and total pore volume were observed in $\text{Fe}_3\text{O}_4@\text{MCM-41}@\text{Zr}$ supported materials. Consequently, it could be concluded that well-organized mesoporous $\text{Fe}_3\text{O}_4@\text{MCM-41}@\text{Zr-piperazine-MNPs}$ catalyst with a high surface area could be obtained in the present study.

3.1.4 | Transmission electron microscopy (TEM) analysis

The TEM images of the prepared functionalized $\text{Fe}_3\text{O}_4@\text{MCM-41}@\text{Zr-MNPs}$ are shown in Figure 5. The

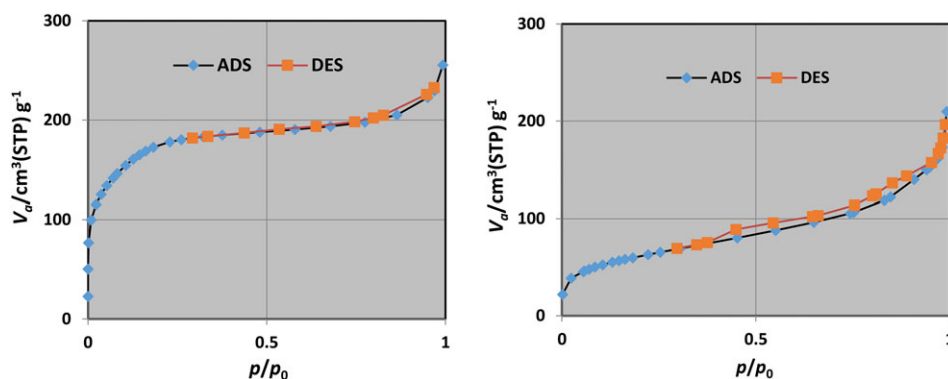


FIGURE 4 The N_2 adsorption/desorption isotherm of a) $\text{Fe}_3\text{O}_4@\text{MCM-41}@\text{Zr-MNPs}$ and b) $\text{Fe}_3\text{O}_4@\text{MCM-41}@\text{Zr-piperazine-MNPs}$

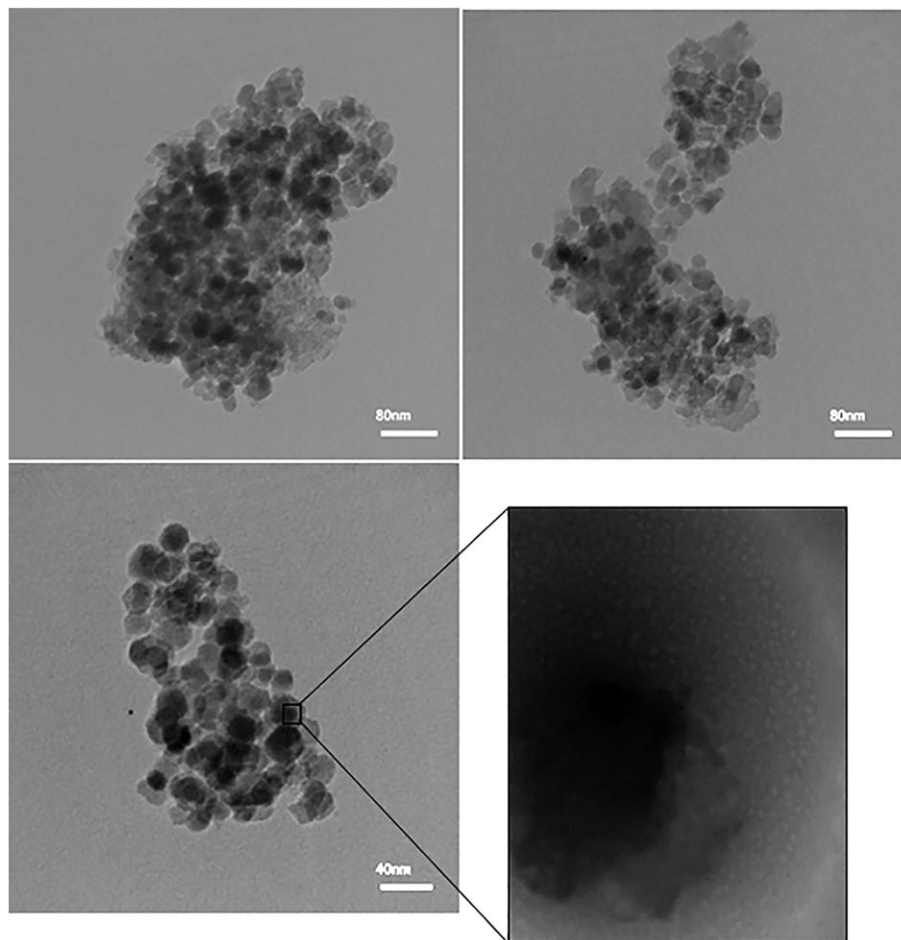


FIGURE 5 The TEM images of $\text{Fe}_3\text{O}_4@\text{MCM-41}@\text{Zr-piperazine-MNPs}$

TEM images disclosed the spherical-like particles of all samples including agglomeration of dark MNPs cores surrounded by lighter amorphous silica shells bearing metals nanoparticles.^[50,64]

3.1.5 | EDX analysis

The EDX results of $\text{Fe}_3\text{O}_4@\text{MCM-41}@\text{Zr-piperazine-MNPs}$ are depicted in Figure 6 indicating the presence of all expected elements (Fe, Si, Zr, N and O). The existence of Zr and N elements demonstrates the successful loading of Zr and piperazine in the next step, onto the surface of the materials.

3.1.6 | TGA analysis

Thermogravimetric analysis (TGA) was performed for characterization of $\text{Fe}_3\text{O}_4@\text{MCM-41}@\text{Zr-MNPs}$ in comparison with $\text{Fe}_3\text{O}_4@\text{MCM-41}@\text{Zr-piperazine-MNPs}$ [Figure 7 (a,b)].

Since more than 90% of the structure of $\text{Fe}_3\text{O}_4@\text{MCM-41}@\text{Zr-MNPs}$ consists of iron, silica, and

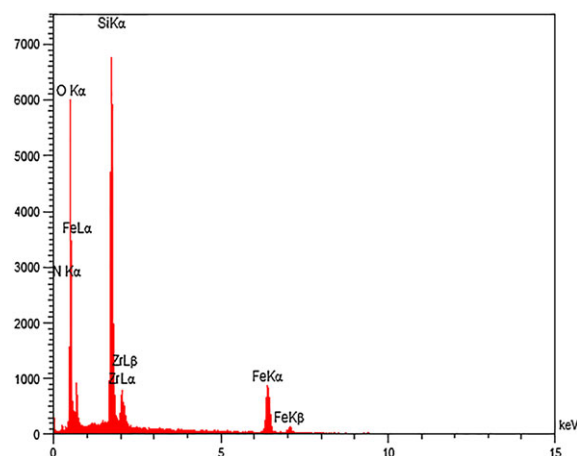


FIGURE 6 The EDX profiles of $\text{Fe}_3\text{O}_4@\text{MCM-41}@\text{Zr-piperazine-MNPs}$

zirconium, so there will be no particular weight loss in this range of temperature and the observed change can be related to the desorption of the physically adsorbed water and removal of OH groups of the MCM network. However, in the case of $\text{Fe}_3\text{O}_4@\text{MCM-41}@\text{Zr-piperazine-MNPs}$, due to the addition of piperazine as an organic

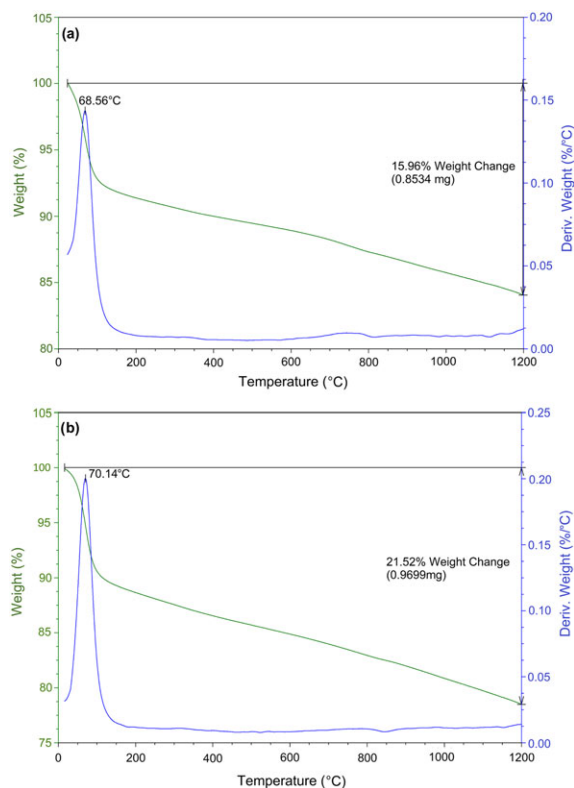


FIGURE 7 The TGA curves of a) $\text{Fe}_3\text{O}_4@\text{MCM-41}@\text{Zr-MNPs}$ and b) $\text{Fe}_3\text{O}_4@\text{MCM-41}@\text{Zr-piperazine-MNPs}$

compound, a larger weight loss is observed, which confirms the catalyst structure.

3.1.7 | VSM analysis

Figure 8 represents the obtained magnetic hysteresis curves of MNPs. Both $\text{Fe}_3\text{O}_4@\text{MCM-41}@\text{Zr-MNPs}$ and $\text{Fe}_3\text{O}_4@\text{MCM-41}@\text{Zr-piperazine-MNPs}$ exhibit typical

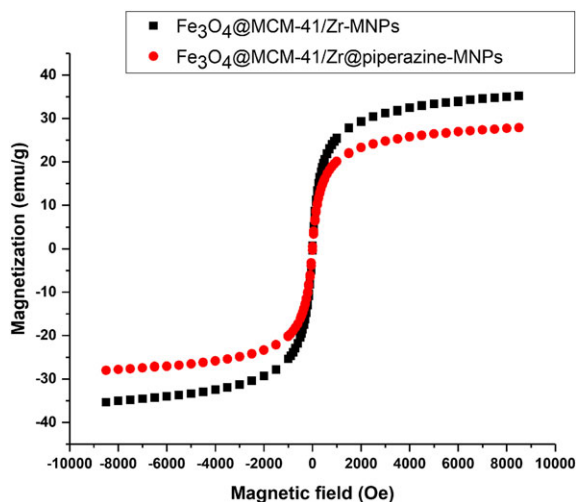


FIGURE 8 The Magnetic hysteresis curves of $\text{Fe}_3\text{O}_4@\text{MCM-41}@\text{Zr-MNPs}$ and $\text{Fe}_3\text{O}_4@\text{MCM-41}@\text{Zr-piperazine-MNPs}$

superparamagnetic behavior, as evidenced by a zero remanence and coercivity on the magnetization loop.^[55]

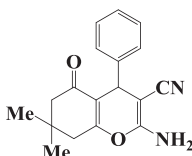
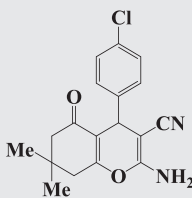
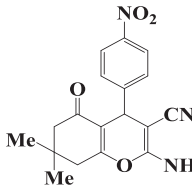
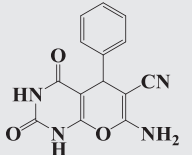
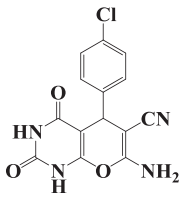
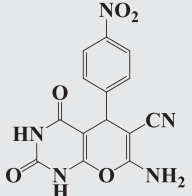
The large saturation magnetization values of $\text{Fe}_3\text{O}_4@\text{MCM-41}@\text{Zr-MNPs}$ and $\text{Fe}_3\text{O}_4@\text{MCM-41}@\text{Zr-piperazine-MNPs}$ were 27.85 emu/g and 35.21 emu/g, respectively, which is sufficiently high for magnetic separation using a conventional magnet. It is deduced that the decrease in saturation magnetization of $\text{Fe}_3\text{O}_4@\text{MCM-41}@\text{Zr-piperazine-MNPs}$ is due to the grafted nonmagnetic organic group, piperazine.

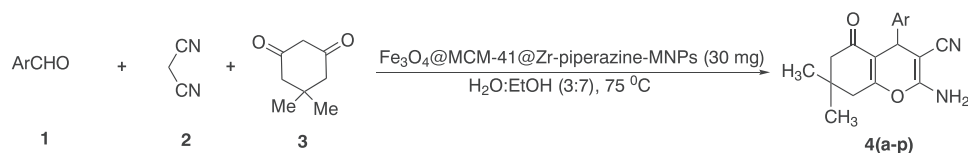
3.2 | Catalytic activity

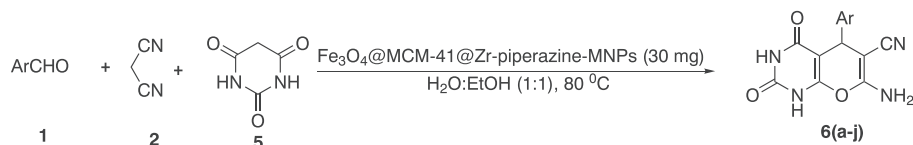
After identification of the prepared MNPs, the synthesized magnetic catalysts were used to promote the synthesis of tetrahydro-4*H*-chromene and pyrano[2,3-*d*]pyrimidinone derivatives. At first, the efficiency of $\text{Fe}_3\text{O}_4@\text{MCM-41}@\text{Zr}$ in the synthesis of 2-amino-4-(4-chlorophenyl)-7,7-dimethyl-5-oxo-5,6,7,8-tetrahydro-4*H*-chromene-3-carbonitrile, 7-amino-5-(4-bromophenyl)-2,4-dioxo-1,3,4,5-tetrahydro-2*H*-pyrano[2,3-*d*]pyrimidine-6-carbonitrile and some other derivatives was surveyed under optimized conditions tabulating in Table 1. Due to the weak obtained results of these reactions that were lower than expected and in order to improve the mentioned reactions to proceeding more efficiently, we decided to investigate the influence of $\text{Fe}_3\text{O}_4@\text{MCM-41}@\text{Zr}$ functionalized with piperazine in the aforementioned first two syntheses. In this regard, to prepare these products in a more efficient way with minimum amount of the catalyst and generally for optimization of the reaction conditions, the reaction of 4-chlorobenzaldehyde **1** (1 mmol), malononitrile **2** (1.2 mmol), and dimedone **3** (1 mmol) or barbituric acid **5** (1 mmol) was selected as a model reaction and the various conditions including amounts of the catalyst, solvent and temperature were examined. Finally, the best conditions are selected on the basis of these results as represented in Schemes 1 and 2. Any further increase of the catalyst or temperature did not improve the reactions times and yields. The obtained results were tabulated in Tables 2 and 3.

In order to generalize the best conditions, different derivatives of tetrahydro-4*H*-chromene (4a-p) and pyrano[2,3-*d*]pyrimidinone (6a-j) were prepared and the results were summarized in Table 4. After ending the reaction, a small amount of products wasted through the work-up process and percentage yields got less than conversion yields. By comparison of the mass of pure product, we got from the chemical reaction (actual yield) and the theoretical maximum (predicted) yield which was calculated from the balanced equation, the percentage of product efficiency (percentage yield) was calculated. Importantly, note that the superparamagnetic nature of

TABLE 1 Preparation of tetrahydro-4*H*-chromene and pyrano[2,3-*d*]pyrimidinone derivatives by using Fe₃O₄@MCM-41@Zr-MNPs as the catalyst

Entry	Aldehyde	Product	Time (min)	Yield (%) ^a	
1	C ₆ H ₅ CHO		4a ^b	40	74
2	4-ClC ₆ H ₄ CHO		4b ^{bv}	30	85
3	4-NO ₂ C ₆ H ₄ CHO		4g ^b	25	82
4	C ₆ H ₅ CHO		6a ^c	35	70
5	4-ClC ₆ H ₄ CHO		6b ^c	20	78
6	4-NO ₂ C ₆ H ₄ CHO		6g ^c	30	80

^aPercentage yield = [actual yield (e.g. in grams)/ predicted theoretical yield (same mass units as above)] x 100.^bThe reaction was done *via* condensation of aldehyde (1 mmol), malononitrile (1.2 mmol), dimedone (1 mmol), and Fe₃O₄@MCM-41@Zr nanocatalyst (0.03 g) in 3 ml aqueous ethanol (3:7) at 75 °C.^cThe reaction was done *via* condensation of aldehyde (1 mmol), malononitrile (1.2 mmol), barbituric acid (1 mmol), and Fe₃O₄@MCM-41@Zr nanocatalyst (0.03 g) in 3 ml aqueous ethanol (1.5:1.5) at 80 °C.**SCHEME 1** Synthesis of tetrahydro-4*H*-chromene derivatives catalyzed by Fe₃O₄@MCM-41@Zr-piperazine-MNPs in aqueous ethanol (3:7) at 75 °C



SCHEME 2 Synthesis of pyrano[2,3-*d*]pyrimidinone derivatives catalyzed by $\text{Fe}_3\text{O}_4@\text{MCM-41}@\text{Zr-piperazine-MNPs}$ in aqueous ethanol (1:1) at 80 °C

TABLE 2 Optimization of the amount of the catalyst, temperature and solvent in the synthesis of tetrahydro-4*H*-chromene derivative of 4-chlorobenzaldehyde

Entry	Amount of catalyst (g)	Solvent	Temp. (°C)	Time (min)	Conversion
1	0.03	H ₂ O	75	60	100
2	0.03	C ₂ H ₅ OH	75	30	100
3	0.03	C ₂ H ₅ OH: H ₂ O (1:1)	75	20	100
4	0.03	C ₂ H ₅ OH: H ₂ O (3:7)	75	30	100
5	0.03	C ₂ H ₅ OH: H ₂ O (7:3)	75	10	100
6	0.03	CH ₃ COCH ₃ : H ₂ O (1:1)	r.t	60	70
7	0.03	H ₂ O	r.t	60	50
8	0.03	C ₂ H ₅ OH	r.t	100	100
9	0.02	C ₂ H ₅ OH	75	25	98
10	0.03	C ₂ H ₅ OH: H ₂ O (2:1)	90	32	100
11	0.04	C ₂ H ₅ OH: H ₂ O (7:3)	75	5	98

TABLE 3 Optimization of the amount of the catalyst, temperature and solvent in the synthesis of pyrano[2,3-*d*]pyrimidinone derivative of 4-chlorobenzaldehyde

Entry	Amount of catalyst (g)	Solvent	Temp. (°C)	Time (min)	Conversion
1	0.03	H ₂ O	80	35	100
2	0.03	C ₂ H ₅ OH	80	25	97
3	0.03	C ₂ H ₅ OH: H ₂ O (1:1)	80	5	100
4	0.03	C ₂ H ₅ OH: H ₂ O (3:7)	r.t	60	70
5	0.04	C ₂ H ₅ OH: H ₂ O (7:3)	80	20	90
6	0.02	CH ₃ COCH ₃ : H ₂ O (1:1)	80	60	50

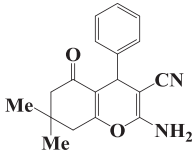
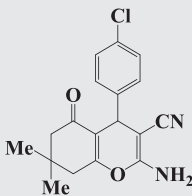
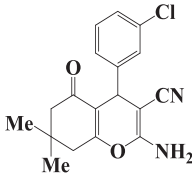
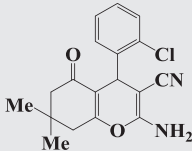
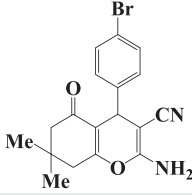
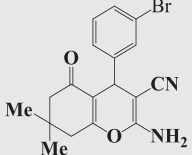
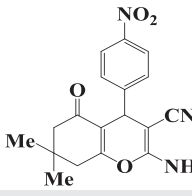
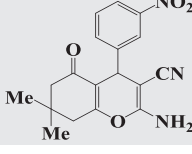
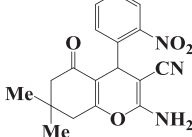
the synthesized nanocatalyst, as a beneficial and valuable feature, made the isolation and reuse of this catalyst very easy. As is shown in Figure 9, in the presence of an external magnet, $\text{Fe}_3\text{O}_4@\text{MCM-41}@\text{Zr-piperazine-MNPs}$ was easily separated from its aqueous suspension in a few minutes.

However, as indicated in Table 4, aromatic aldehydes with electron-withdrawing groups reacted as well as aromatic aldehydes with electron-releasing groups. So the different group substitution of the aldehydes with the same groups located at different positions of the aromatic

ring has been shown not to have much effect on the formation of the final product.

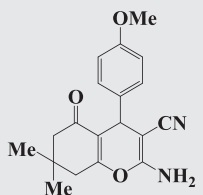
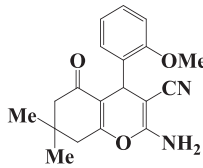
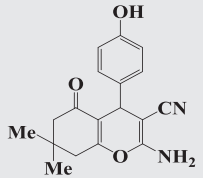
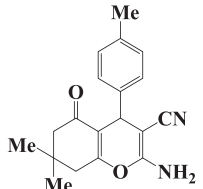
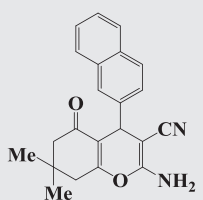
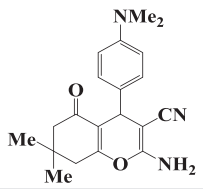
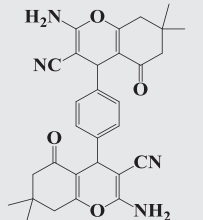
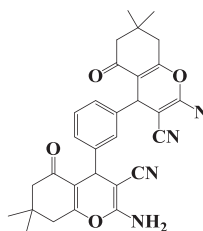
It's notable that after completion of the reaction, as indicated by TLC (*n*-hexane: ethyl acetate; 6:4 (the mixture was dissolved in sufficient amount of ethanol in order to dissolve all of the chemical product which results in the presence of insoluble solid catalyst particles. Then in the presence of a magnetic stirrer bar, the superparamagnetic nanocatalyst was separated and the reaction mixture turned clear. Complete and accurate matching of the melting point range with what

TABLE 4 Preparation of tetrahydro-4*H*-chromene and pyrano[2,3-*d*]pyrimidinone derivatives by using Fe₃O₄@MCM-41@Zr-piperazine-MNPs as the catalyst

Entry	Aldehyde	Product	Time (min)	Yield (%) ^a	M. p. (°C)		[Ref.]	
					Found	Reported		
1	C ₆ H ₅ CHO		4a ^b	10	81	227-229	225-228	[13]
2	4-ClC ₆ H ₄ CHO		4b ^b	10	90	207-209	208-210	[13]
3	3-ClC ₆ H ₄ CHO		4c ^b	20	87	229-232	230-233	[13]
4	2-ClC ₆ H ₄ CHO		4d ^b	5	89	216-218	213-215	[13]
5	4-BrC ₆ H ₄ CHO		4e ^b	15	88	201-203	199-201	[13]
6	3-BrC ₆ H ₄ CHO		4f ^b	20	89	225-227	227-229	[14]
7	4-NO ₂ C ₆ H ₄ CHO		4g ^b	6	85	178-179	176-179	[13]
8	3-NO ₂ C ₆ H ₄ CHO		4h ^b	10	84	202-204	202-205	[13]
9	2-NO ₂ C ₆ H ₄ CHO		4i ^b	4	92	218-219	213-217	[13]

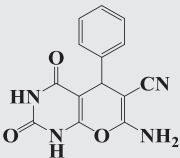
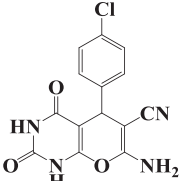
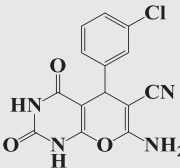
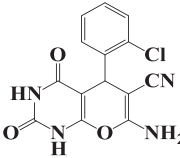
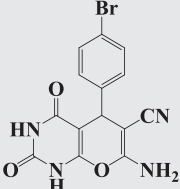
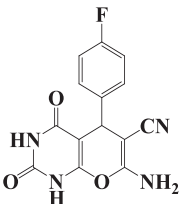
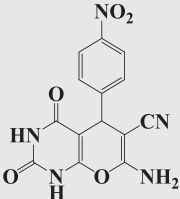
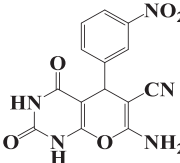
(Continues)

TABLE 4 (Continued)

Entry	Aldehyde	Product		Time (min)	Yield (%) ^a	M. p. (°C)		[Ref.]
						Found	Reported	
10	4-MeOC ₆ H ₄ CHO		4j ^b	20	88	196-198	200-204	[13]
11	2-MeOC ₆ H ₄ CHO		4k ^b	20	82	203-265	198-203	[13]
12	4-OHC ₆ H ₄ CHO		4l ^b	35	86	208-210	210-214	[13]
13	4-MeC ₆ H ₄ CHO		4m ^b	8	85	215-217	211-214	[13]
14	2-Naphthaldehyde		4mn ^b	45	90	266-268	262-265	[13]
15	4-NMe ₂ C ₆ H ₄ CHO		4n ^b	10	63	202-204	199-203	[13]
16	Terephthalaldehyde		4o ^b	20	84	264-267	266-268	[15]
17	Isophthalaldehyde		4p ^b	40	81	240-242	243-244	[15]

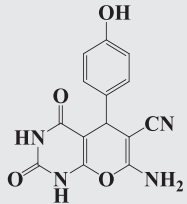
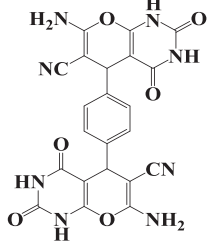
(Continues)

TABLE 4 (Continued)

Entry	Aldehyde	Product		Time (min)	Yield (%) ^a	M. p. (°C)		[Ref.]
						Found	Reported	
18	C ₆ H ₅ CHO		6a ^c	20	90	220-222	219-222	[13]
19	4-ClC ₆ H ₄ CHO		6b ^c	10	90	237-239	238-240	[13]
20	3-ClC ₆ H ₄ CHO		6c ^c	30	91	238-240	240-241	[16]
21	2-ClC ₆ H ₄ CHO		6d ^c	35	85	210-213	209-214	[13]
22	4-BrC ₆ H ₄ CHO		6e ^c	10	88	225-227	227-230	[13]
23	4-FC ₆ H ₄ CHO		6f ^c	30	84	263-246	264-266	[13]
24	4-NO ₂ C ₆ H ₄ CHO		6g ^c	6	92	238-240	237-239	[13]
25	3-NO ₂ C ₆ H ₄ CHO		6h ^c	15	88	260-263	261-264	[13]

(Continues)

TABLE 4 (Continued)

Entry	Aldehyde	Product		Time (min)	Yield (%) ^a	M. p. (°C)		[Ref.]
						Found	Reported	
26	4-OHC ₆ H ₄ CHO		6i ^c	35	59	>300	>300	[13]
27	4-Terephthalaldehyde		6j ^c	25	87	>300	>300	[13]

^aPercentage yield = [actual yield (e.g. in grams)/ predicted theoretical yield (same mass units as above)] x 100.

^bThe reaction was done *via* condensation of aldehyde (1 mmol), malononitrile (1.2 mmol), dimedone (1 mmol), and Fe₃O₄@MCM-41@Zr nanocatalyst (0.03 g) in 3 ml aqueous ethanol (3:7) at 75 °C.

^cThe reaction was done *via* condensation of aldehyde (1 mmol), malononitrile (1.2 mmol), barbituric acid (1 mmol), and Fe₃O₄@MCM-41@Zr nanocatalyst (0.03 g) in 3 ml aqueous ethanol (1.5:1.5) at 80 °C.

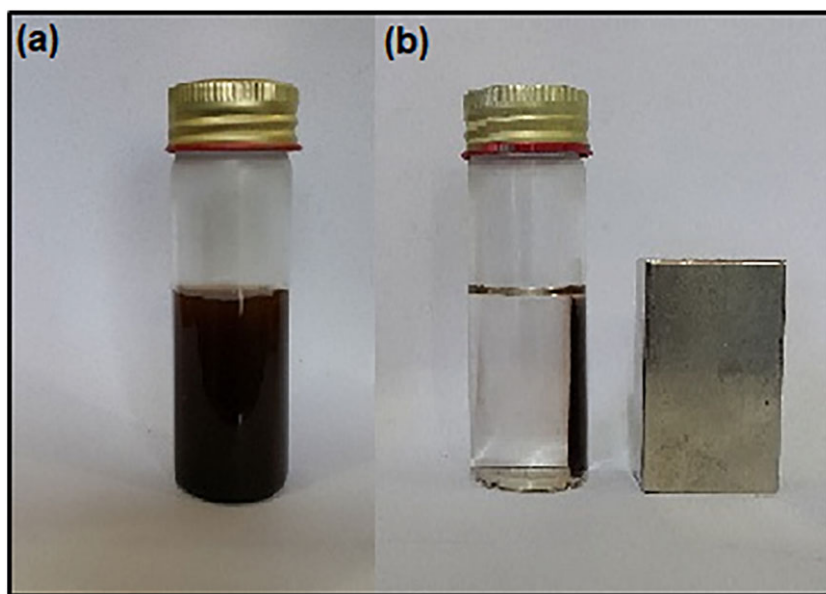


FIGURE 9 Photographs of an aqueous suspension of Fe₃O₄@MCM-41@Zr-piperazine-MNPs before (a) and after (b) magnetic capture

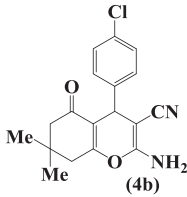
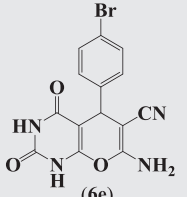
is given in the reference articles is another proof to this matter, however, the presence of nanocatalyst, as impurity in the obtained product, leads to lower the overall melting point of the compound and also increase the range of the melting point value. Additionally, checking the results of ¹HNMR and ¹³CNMR analysis of the obtained product ensure us not remaining the nanocatalyst which has an organic functional group like piperazine.

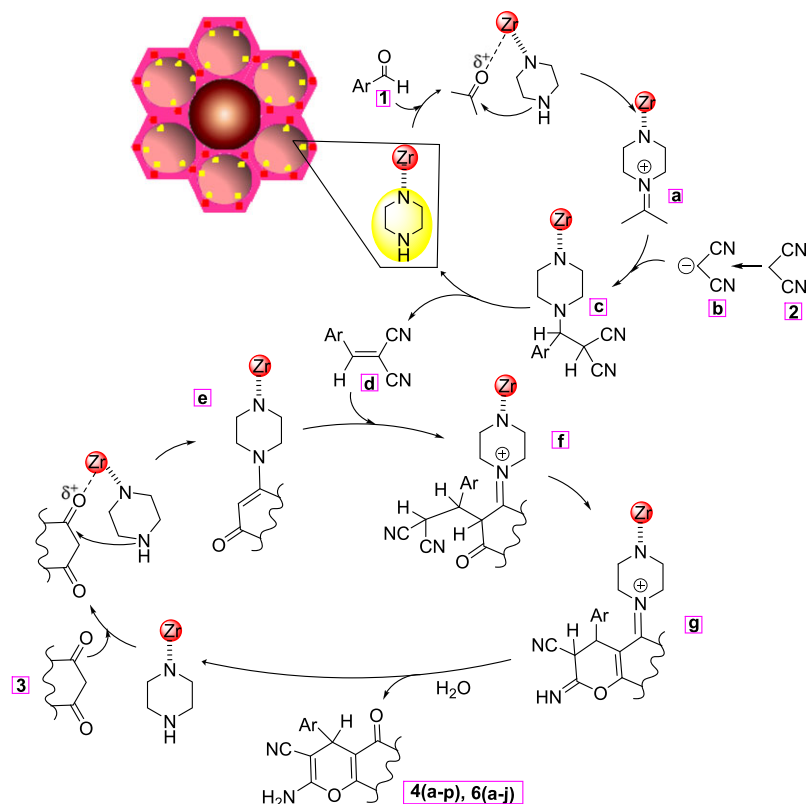
In order to reveal the competence of the catalyst, it was essential to compare the catalytic efficiency of Fe₃O₄@MCM-41@Zr-piperazine-MNPs with previous methods. Thus the synthesis of 2-amino-4-(4-chlorophenyl)-7,7-dimethyl-5-oxo-5,6,7,8-tetrahydro-4H-chromene-3-carbonitrile 4b (entry 2, Table 4) and 7-amino-5-(4-bromophenyl)-2,4-dioxo-1,3,4,5-tetrahydro-2H-pyrano[2,3-d]pyrimidine-6-carbonitrile 6j (entry 22, Table 4) was mentioned as model reactions with the

selected catalysts and the results were presented in Table 5. With an overall look at Table 5, we can perceive that not only our method is the best choice comparing to

other mentioned catalytic systems in terms of yield and reaction time, but also high activity, low consumption of organic solvents, compatibility with environment and

TABLE 5 Comparison of the efficiency of $\text{Fe}_3\text{O}_4@\text{MCM-41}@\text{Zr-piperazine-MNPs}$ with other reported catalysts in the studied reactions

Entry	Product	Catalyst	Amount	Condition	Time (min)	Yield (%)	[Ref.]
1	 (4b)	N-Methylimidazole	(0.2 mol)	$\text{C}_2\text{H}_5\text{OH}$ / r.t.	60	95	[16]
2		TMAH	(0.1 mol)	H_2O / r.t.	30–120	83	[8]
3		(S)-proline	(0.5 mol)	H_2O / r.t.	120	97	[65]
4		Na_2SeO_4	(0.1 g)	H_2O : $\text{C}_2\text{H}_5\text{OH}$ (1:1) / reflux	180	90	[66]
5		HDMBAB	(0.12 mol)	H_2O / 80–90 °C	7.5	90	[67]
6		Tetrabutylammonium bromide (TBAB)	(0.1 mol)	H_2O / reflux	30	95	[29]
7	 (6e)	$\text{Fe}_3\text{O}_4@\text{SiO}_2$ / DABCO	(0.05 g)	H_2O / 80 °C	25	90	[13]
8		p-Dodecylbenzenesulfonic acid	(4×10^{-4}) mol	H_2O / reflux	240	69	[19]
9		(Diacetoxyiodo)benzene	(0.05 mol)	H_2O : $\text{C}_2\text{H}_5\text{OH}$ (1:1) / reflux	30	89	[25]
10		$[\text{H}_2\text{-DABCO}][\text{H}_2\text{PO}_4]_2$	(0.05 g)	H_2O : $\text{C}_2\text{H}_5\text{OH}$ (1:2) / reflux	15	95	[35]
11		$\text{KAl}(\text{SO}_4)_2 \cdot 12\text{H}_2\text{O}$ (alum)	(0.1 mol)	H_2O / 80 °C	40	93	[28]
12		$\text{Fe}_3\text{O}_4@\text{MCM-41}@\text{Zr-Piperazine}$	(0.03 g)	H_2O : $\text{C}_2\text{H}_5\text{OH}$ (7:3) / reflux	10	90	[This work]
13		Diammonium hydrogen phosphate	(0.1 mol)	H_2O : $\text{C}_2\text{H}_5\text{OH}$ (1:1) / r.t.	120	81	[26]
14		L-Proline	(0.05 mol)	H_2O : $\text{C}_2\text{H}_5\text{OH}$ (1:1) / r.t.	90	75	[27]
15		$\text{KAl}(\text{SO}_4)_2 \cdot 12\text{H}_2\text{O}$ (alum)	(0.1 mol)	H_2O / 80 °C	30	85	[28]
16		Tetrabutylammonium bromide (TBAB)	(0.1 mol)	H_2O / reflux	25	85	[29]
17		$[\text{DABCO}](\text{SO}_3\text{H})_2(\text{HSO}_4)_2$	(2×10^{-5}) mol	H_2O / reflux	5	87	[16]
18		$\text{Fe}_3\text{O}_4@\text{MCM-41}@\text{Zr-piperazine}$	(0.03 g)	H_2O : $\text{C}_2\text{H}_5\text{OH}$ (1:1) / 80 °C	10	90	[This work]



SCHEME 3 A plausible mechanism for the preparation of tetrahydro-4H-chromene **4** and pyrano[2,3-d]pyrimidinone **6** derivatives

easy separation *via* an external magnetic field are some superiorities of our new proposed catalyst. As shown in this table, $\text{Fe}_3\text{O}_4\text{@MCM-41@Zr-piperazine-MNPs}$ can be proposed as a useful catalyst in terms of compatibility with the environment, yields of the products and reaction times compared to the other reported systems.

A conceivable mechanism of the catalyst working in the reaction is outlined in Scheme 3. Accordingly, we suggest that $\text{Fe}_3\text{O}_4\text{@MCM-41@Zr-piperazine-MNPs}$ is an effective catalyst for the generation of iminium ion (**a**) which its higher reactivity compared to the carbonyl group species is utilized to facilitate the Knoevenagel condensation between aryl aldehyde **1** and anionic form of malononitrile **2** (through H adsorption by piperazine), which proceeds *via* intermediate (**c**) and, after dehydration, olefin (**d**) is produced. $\text{Fe}_3\text{O}_4\text{@MCM-41@Zr-piperazine-MNPs}$ also catalyzes the formation of a proposed enamine intermediate (**e**) from β -diketone **3**, which reacts with the cyano olefin (**d**) *via* a nucleophilic addition to produce intermediate (**f**) followed by an

intramolecular cyclization and tautomerization to give the iminium ion (**g**); upon hydrolysis of this ion the product **4** can be formed.

3.3 | Reusability of the catalyst

To investigate the activity constancy of the catalyst, the catalyst was reused five times in the synthesis of 2-amino-4-(4-chlorophenyl)-7,7-dimethyl-5-oxo-5,6,7,8-tetrahydro-4*H*-chromene-3-carbonitrile **4b** (entry 2, Table 4) and 7-amino-5-(4-chlorophenyl)-2,4-dioxo-1,3,4,5-tetrahydro-2*H*-pyrano[2,3-*d*]pyrimidine-6-carbonitrile **6b** (entry 19, Table 4) under both the best reactions conditions. The catalyst was magnetically recovered after each run, washed with ethanol, dried in air prior to use and tested for its activity in the subsequent run. This procedure was repeated 5 times for both reactions and each time the mentioned product was obtained by the recovered catalyst with the slight change in the reaction time and yield as shown in Figures 10 and 11.

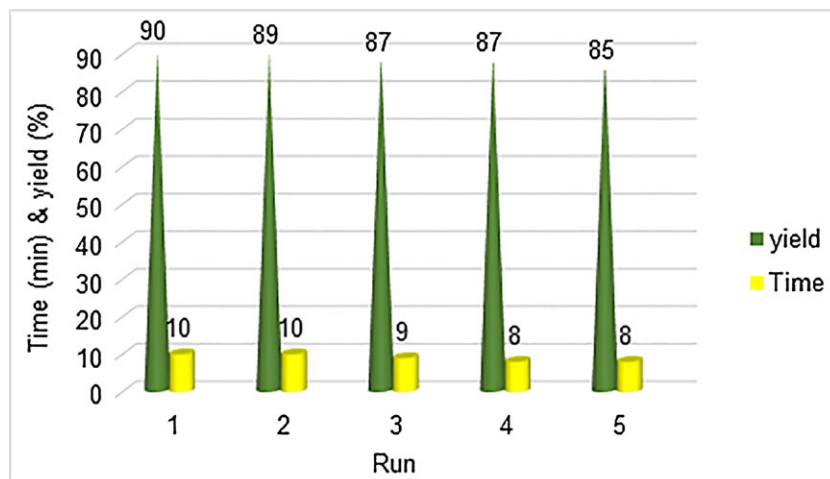


FIGURE 10 Reusability of $\text{Fe}_3\text{O}_4\text{@MCM-41@Zr-piperazine-MNPs}$ in the synthesis of 2-amino-4-(4-chlorophenyl)-7,7-dimethyl-5-oxo-5,6,7,8-tetrahydro-4*H*-chromene-3-carbonitrile **4b**

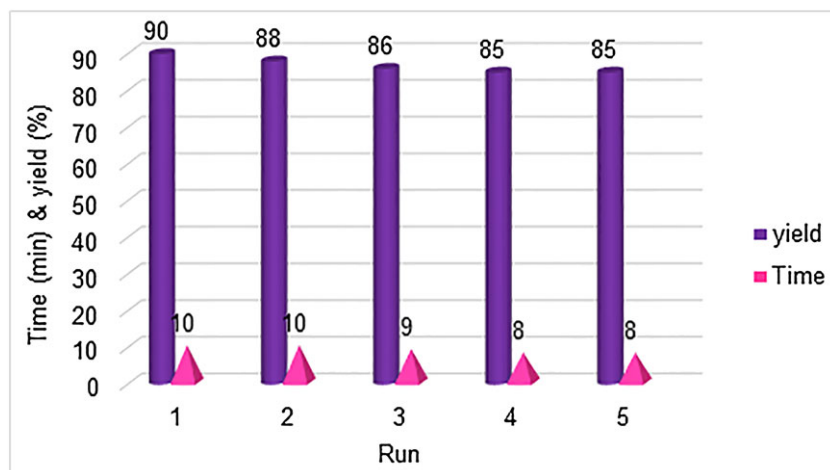


FIGURE 11 Reusability of $\text{Fe}_3\text{O}_4\text{@MCM-41@Zr-piperazine-MNPs}$ in the synthesis of 7-amino-5-(4-chlorophenyl)-2,4-dioxo-1,3,4,5-tetrahydro-2*H*-pyrano[2,3-*d*]pyrimidine-6-carbonitrile **6b**

4 | CONCLUSION

In conclusion, based on different represented analyses, Fe₃O₄@MCM-41@Zr modified with piperazine, as a new stable and highly active catalyst, has been synthesized successfully and surveyed its capability in preparing a variety of tetrahydro-4H-chromene and pyrano[2,3-d]pyrimidinone derivatives under mild conditions. The green conditions, excellent yields, practicability, operational simplicity, product purity, cost efficiency and environmentally profits are the considerable advantages of this protocol. According to these observations, it could be deduced that this green, recyclable and cost-effective catalyst, with simple experimental and work-up procedure, makes it a useful alternative to the previous methodologies for the scale-up of these one-pot three-component reactions.

ACKNOWLEDGEMENTS

We are thankful to the Research Council of the University of Guilan for the partial support of this research.

ORCID

Farhad Shirini  <http://orcid.org/0000-0002-0768-3241>

REFERENCES

- [1] V. Polshettiwar, R. S. Varma, *Green Chem.* **2010**, *12*, 743.
- [2] G. Q. Lu, X. S. Zhao, UK: Imperial College Press. **2004**, 4.
- [3] M. Sharifi, J. Schneider, M. Wark, *Microporous Mesoporous Mater.* **2012**, *151*, 506.
- [4] A. I. Carrillo, E. Serrano, R. Luque, J. Garcia-Martinez, *Appl. Catal. A* **2013**, *483*, 383.
- [5] T. Conesa, R. Mokaya, J. M. Campelo, A. A. Romero, *Chem. Commun.* **2006**, *17*, 1839.
- [6] D. Kumar, K. Schumacher, C. du Fresne von Hohenesche, M. Grün, K. K. Unger, *Colloid. Surface. A* **2001**, *187*, 109.
- [7] N. I. Cuello, V. R. Elías, C. E. Rodriguez Torres, M. E. Crivello, M. I. Oliva, G. A. Eimer, *Microporous Mesoporous Mater.* **2015**, *203*, 106.
- [8] J. Davarpanah, A. R. Kiasat, S. Noorizadeh, M. Ghahremani, *J. Mol. Catal. A: Chem.* **2013**, *376*, 78.
- [9] X. Z. Lian, Y. Huang, Y. Q. Li, W. J. Zheng, *Monatsh. Chem.* **2008**, *139*, 129.
- [10] M. Khoobi, L. Ma'mani, F. Rezazadeh, Z. Zareie, A. Foroumadi, A. Ramazani, A. Shafiee, *J. Mol. Catal. A: Chem.* **2012**, *359*, 74.
- [11] E. Sheikhhosseini, D. Ghazanfari, V. Nezamabadi, *Iran. J. Catal.* **2013**, *3*, 197.
- [12] S. Balalaie, M. Sheikh-Ahmadi, M. Bararjanian, *Catal. Commun.* **2007**, *8*, 1724.
- [13] S. R. Kamat, A. H. Mane, S. M. Arde, R. S. Salunkhe, *IJPCBS.* **2014**, *4*, 1012.
- [14] J. Albadi, A. Mansourneshad, T. Sadeghi, *Res. Chem. Intermed.* **2015**, *41*, 8317.
- [15] H. Kefayati, M. Valizadeh, A. Islamnezhad, *Electrochemistry* **2014**, *6*, 80.
- [16] A. Alizadeh, M. M. Khodaei, M. Beygzadeh, D. Kordestani, M. Feyzi, *Bull. Korean Chem. Soc.* **2012**, *33*, 2546.
- [17] M. Seifi, H. Sheibani, *Catal. Lett.* **2008**, *126*, 275.
- [18] S. Gurumurthi, V. Sundari, R. Valliappan, *J. Chem.* **2009**, *6*, S466.
- [19] J. Zheng, Y. Q. Li, *Appl. Sci. Res.* **2011**, *3*, 381.
- [20] J. Albadi, M. Fadaeian, F. A. Balout-Bangan, *Iran. J. Org. Chem.* **2013**, *5*, 1089.
- [21] M. G. Dekamin, M. Eslami, A. Maleki, *Tetrahedron* **2013**, *69*, 1074.
- [22] A. R. Moosavi-Zare, M. A. Zolfigol, O. Khaledian, V. Khakyzadeh, M. D. Farahani, H. G. Kruger, *New J. Chem.* **2014**, *38*, 2342.
- [23] H. Hu, F. Qiu, A. Ying, J. Yang, H. Meng, *Int. J. Mol. Sci.* **2014**, *15*, 6897.
- [24] N. Hazeri, M. T. Maghsoodlou, F. Mir, M. Kangani, H. Saravani, E. Molashahi, *Chin. J. Catal.* **2014**, *35*, 391.
- [25] A. S. Waghmare, S. S. Pandit, *Iran. Chem. Commun.* **2015**, *3*, 291.
- [26] S. Balalaie, S. Abdolmohammadi, H. R. Bijanzadeh, A. M. Amani, *Mol. Diversity* **2008**, *12*, 85.
- [27] M. Bararjanian, S. Balalaie, B. Movassagh, A. M. Amani, *J. Iran. Chem. Soc.* **2009**, *6*, 436.
- [28] A. Mobinikhaledi, N. Foroughifar, M. A. B. Fard, *Chem* **2010**, *40*, 179.
- [29] A. Mobinikhaledi, M. A. B. Fard, *Acta Chim. Slov.* **2010**, *57*, 931.
- [30] J. Azizian, A. Shameli, S. Balalaie, M. M. Ghanbari, S. Zomorodbakhsh, M. Entezari, S. Bagheri, G. Fakhrpour, *Orient. J. Chem.* **2012**, *28*, 327.
- [31] G. M. Ziarani, S. Faramarzi, S. Asadi, A. Badiei, R. Bazl, M. Amanlou, *DARU J. Pharm. Sci* **2013**, *21*, 3.
- [32] B. Sabour, M. H. Peyrovi, M. Hajimohammadi, *Res. Chem. Intermed.* **2015**, *41*, 1343.
- [33] B. Sadeghi, M. Bouslik, M. R. Shishehbore, *J. Iran. Chem. Soc.* **2015**, *12*, 1801.
- [34] O. Goli-Jolodar, F. Shirini, M. Seddighi, *J. Iran. Chem. Soc.* **2016**, *13*, 457.
- [35] F. Shirini, M. Safarpour, N. L. N. Daneshvar, *J. Mol. Liq.* **2017**, *234*, 268.
- [36] B. M. Trost, in *Transition Met. Org. React. WILEY-VCH Verlag GmbH, D-69469*, (Eds: M. Beller, C. Bolm), Weinheim, Germany **1998**.
- [37] A. K. Chakraborti, R. Gulhane, *Synlett* **2004**, *4*, 627.
- [38] S. Z. M. Shamshuddin, *Synlett* **2005**, *2*, 361.
- [39] M. Beller, C. Bolm, *Transition Met. Org Synth*, 2nd ed., Wiley-VCH, Weinheim **2004**.
- [40] C. M. Vogels, S. A. Westcott, *Curr. Org. Chem.* **2005**, *9*, 687.
- [41] B. C. G. Soderberg, *Coord. Chem. Rev.* **2004**, *248*, 1085.

- [42] Z. H. Zhang, T.-S. Li, *Current Org. Chem.* **2009**, *13*, 1.
- [43] X. X. Wang, F. Lefebvre, P. Patarin, J. M. Basset, *Microporous Mesoporous Mater.* **2001**, *42*, 269.
- [44] X. Yang, L. Zhou, C. Chen, J. Xu, *Mater. Chem. Phys.* **2010**, *120*, 42.
- [45] W.-H. Zhang, J.-L. Shi, L.-Z. Wang, D.-S. Yan, *Mater. Lett.* **2000**, *46*, 35.
- [46] F. Shirini, M. A. Zolfigol, E. Mollarazi, *Synth. Commun.* **2006**, *36*, 2307.
- [47] F. Shirini, M. A. Zolfigol, A. Pourhabib, *Russ. J. Org. Chem.* **2003**, *39*, 1191.
- [48] F. Shirini, M. A. Zolfigol, E. Mollarazi, *Synth. Commun.* **2005**, *35*, 1541.
- [49] F. Shirini, M. A. Zolfigol, A. Safari, *J. Chem. Res (S)*. **2006**, 154.
- [50] N. Saadatjoo, M. Golshekan, S. Shariati, H. Kefayati, P. Azizi, *J. Mol. Catal. A: Chem.* **2013**, *377*, 173.
- [51] Y. C. Chien, H. P. Wang, S. H. Liu, T. L. Hsiung, H. S. Tai, C. Y. Peng, *J. Hazard. Mater.* **2008**, *151*, 461.
- [52] F. M. Yang, L. Chen, C. T. Au, S. F. Yin, *Environ. Prog. & Sustainable Energy* **2015**, *34*, 1814.
- [53] M. B. Yue, Y. Chun, Y. Cao, X. Dong, J. H. Zhu, *Adv. Funct. Mater.* **2006**, *16*, 1717.
- [54] A. Pradeep, G. Chandrasekaran, *Mater. Lett.* **2006**, *60*, 371.
- [55] H. Kefayati, M. Golshekan, S. Shariati, M. Bagheri, *Chin. J. Catal.* **2015**, *36*, 572.
- [56] W. Que, Y. Zhou, Y. L. Lam, Y. C. Chan, C. H. Kam, *Thin Solid Films* **2000**, *358*, 16.
- [57] A. V. Rao, R. R. Kalesh, G. M. Pajonk, *J. Mater. Sci.* **2003**, *38*, 4407.
- [58] S. Ghodke, R. Patel, U. Chudasama, *IJIRSET*. **2015**, *4*, 18735.
- [59] O. Alver, C. Parlak, M. Senyel, *Spectrochim. Acta Mol. Biomol. Spectrosc.* **2007**, *67*, 793.
- [60] J. H. Jang, H. B. Lim, L. Chou, *Microchem Catal. Sci. Technol.* **2013**, *3*, 1942.
- [61] X. Xu, C. Song, J. M. Andresen, B. G. Miller, A. W. Scaroni, *Energy & Fuels* **2002**, *16*, 1463.
- [62] N. La-Salvia, J. J. Lovón-Quintana, G. P. Valença, *Braz. J. Chem. Eng.* **2015**, *32*, 489.
- [63] L. Lia, S. Yub, F. Liub, J. Yanga, S. Zhaug, *Catal. Lett.* **2005**, *100*, 227.
- [64] M. Abdollahi-Alibeik, G. Ahmadi, *Res. Chem. Intermed.* **2015**, *41*, 8173.
- [65] S. Balalaie, M. Bararjanian, A. M. Amani, B. Movassagh, *Synlett* **2006**, *2*, 263.
- [66] R. Hekmatshoar, S. Majedi, K. Bakhtiari, *Catal. Commun.* **2008**, *9*, 307.
- [67] T. S. Jin, A.-Q. Wang, F. Shi, L.-S. Han, L.-B. Liu, T.-S. Li, *ARKIVOC* **2006**, xiv, 78.

SUPPORTING INFORMATION

Additional Supporting Information may be found online in the supporting information tab for this article.

How to cite this article: Pourhasan-Kisomi R, Shirini F, Golshekan M. Introduction of organic/inorganic Fe₃O₄@MCM-41@Zr-piperazine magnetite nanocatalyst for the promotion of the synthesis of tetrahydro-4H-chromene and pyrano[2,3-d]pyrimidinone derivatives. *Appl Organometal Chem.* 2018;e4371. <https://doi.org/10.1002/aoc.4371>